Potential distribution along gas evolving electrodes*

C. ELSNER‡ , F. COEURET

CNRS-ENSCR, Avenue du Général Leclerc, 35000 Rennes-Beaulieu, France

This paper reports an experimental study of gas-evolving electrodes made of expanded metal. The variations of the cell voltage with the electrolyte velocity and the intensity of the current are studied for different orientations of the mesh with respect to the electrolyte flow direction. Using probes, the solution potential distributions along the electrodes are obtained.

1. Introduction

Relatively few papers are concerned with the behaviour of gas evolving electrodes made of expanded [1–3] or perforated metal [4] with a view to industrial application. The advantage of such electrodes, particularly those of expanded metal, is to deflect the gas bubbles out of the inter-electrode space, thus minimizing the increase of the ohmic potential drop due to the bubbles produced.

The influence of the electrolyte flow velocity on the cell voltage has been studied when the gas evolving electrode is planar [5, 6] or a non-flat perforated structure [4]. It is shown that the thickness of the space free for the electrolyte flow behind the perforated electrode strongly influences the cell voltage [4]. Also, using sectioned electrodes, the distribution of the local current along the height of perforated electrodes has been determined.

The favourable effect of a non-flat expanded electrode on the limitation of the cell voltage has justified the study of the influence of the size and of the orientation of the mesh of the expanded metal when gas evolution occurs on it. Both questions of overall cell voltage and of electrode potential distribution are considered in the present work which concerns the cathodic evolution of hydrogen from aqueous sodium hydroxide within cathodic compartments of small thickness. Other elements of the programme consider the

electrolyte to electrode mass transfer when gas is evolved at the expanded metal electrode and also the current distribution through the thickness of gas evolving electrodes consisting of stacks of sheets of expanded metal [7].

2. Experimental details

2.1. Cell and hydraulic circuit

The cell is parallelepipedic, has two compartments and is made of Altuglas. It is schematically represented in Fig. 1a which shows the position of the expanded metal cathode. This electrode (1, 2 or 3 mm thick) is separated from the transparent wall and from the diaphragm (ion exchange membrane) by a rubber gasket 2 mm thick. The catholyte is distributed at the bottom of the compartment through a rectangular slot existing in the wall, and flows out of the compartment through a similar slot. Four holes in the transparent wall (Fig. 1b) allow Luggin capillaries to be positioned for determination of the solution potential distribution along the electrode height.

The cationic exchange membrane is supported on a planar sheet of sintered polyethylene which is located within a frame of Altuglas. The anodic compartment is a rectangular channel (7.2 cm wide; 17 cm high) the thickness of which (2.6 cm) is sufficiently high for easy removal of the oxygen produced in this compartment.

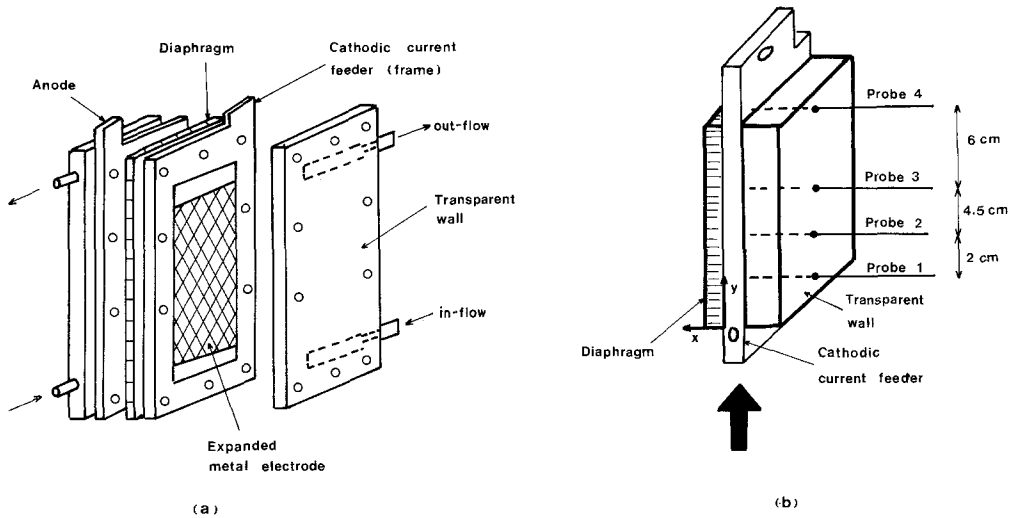Each compartment is part of a specific hydraulic

---

Fig. 1. Schematic views of the cell: (a) location of the expanded metal cathode, (b) positions of the probes in the wall.

circuit which includes a centrifugal pump, valves, a rotameter and a separator for the elimination of the bubbles from the electrolyte out-flow. The electrolyte (catholyte and anolyte) is a 2N NaOH solution which flows in both independent closed circuits; its temperature is maintained equal to 30° C by controlled heating in each tank, while nitrogen is continuously bubbled into the catholyte only.

2.2. Electrodes

The working electrodes (cathodes) are rectangular (dimensions 7 cm × 14 cm) and made of expanded stainless steeel (Z6 CN 1804). Three types of mesh are used; their characteristics, according to the geometric definitions of Figs. 2a and b, are summarized in Table 1 together with the specific surface area, a_s, of a grid and its overall porosity, ϵ_g. Each expanded metal electrode is soldered to a rectangular stainless steel frame, the thickness of which is equal to the apparent thickness e_a of the expanded metal; this frame (see Fig. 1a) is the current feeder to the expanded metal. The mesh of material M_1 and that of M_2 are 'normal'; the third material is of a micromesh type.

The anode is always identical to the cathode when expanded metal is used for the cathode. Planar nickel or stainless steel cathodes are used in some experiments; in such cases the cathode is the
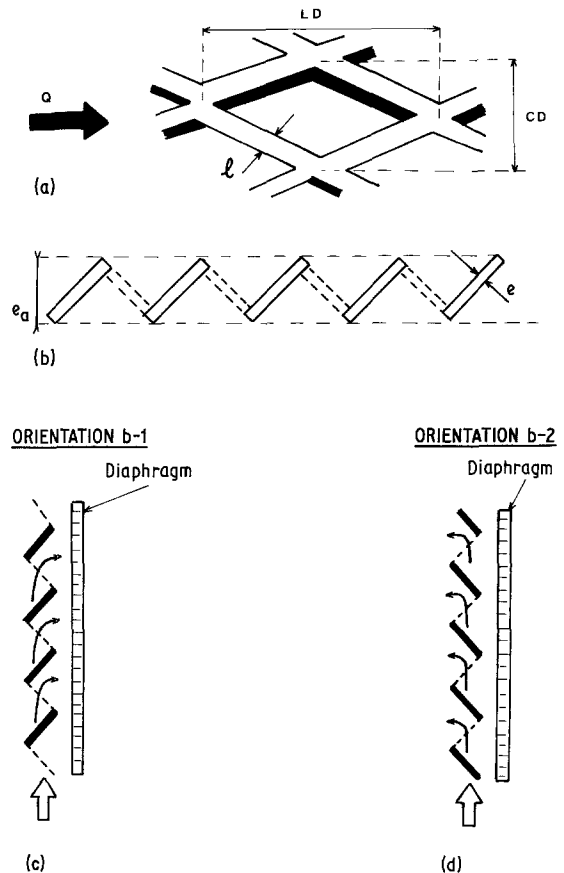

Fig. 2. Description and positioning of the mesh electrode with respect to the general electrolyte flow direction.

Table 1.

Material	LD (cm)	CD (cm)	l (cm)	e (cm)	e_a (cm)	a_s (cm^2 cm^{-3})	ϵ_g
M_1	1.6	0.7	0.2	0.06	0.26	48	0.86
M_2	1.0	0.44	0.1	0.06	0.20	60	0.86
Micromesh	0.6	0.23	0.05	0.02	0.05	174	0.87

wall of the compartment (no flow of electrolyte is possible between the cathode and the transparent wall).

As represented in Fig. 1b, four Luggin capillary probes (Nos. 1 to 4) which are connected to a reference calomel electrode can be introduced through special holes in order to measure at the four corresponding positions, the local solution potential near the surface of the cathode.

Before each experiment the electrodes are washed with deionized water and acetone.

2.3. *Objective and experimental parameters*

The aim of the work is to show the influence of the geometric and hydrodynamic conditions on the cell voltage U_c and on the electrode potential distribution in the vertical direction, measured from probe 1 which is located near the lower part of the cathode (expanded metal or planar sheet of metal) when gas evolution occurs. The electrode geometry (see Table 1), the catholyte flow velocity $\bar{v}_c$ based on the empty channel ($\bar{v}_c = 1, 2, 3$ and 5 cm s^{-1}) and the overall cell current I imposed on the cell ($I = 1, 3, 5, 8$ and 10 A) are the parameters varied in the study. A further geometrical parameter is the orientation of the expanded metal mesh with respect to the general electrolyte flow direction. Three possibilities exist:

orientation (a): the large diagonal, LD, is parallel to the general flow direction (see Fig. 2a).
orientation (b): the small diagonal, CD, (Figs. 2c and d) is parallel to the flow. Two variants b-1 and b-2 have to be considered. Variant b-1 is such that the mixture of gas bubbles and electrolyte is deflected by the expanded metal towards the separator. For variant b-2 the mixture is deflected from the separator and it is hoped that the increase of the apparent electrical resistivity between the gas evolving electrode and the diaphragm will be lower in this case than in variant b-1.

A SODILEC SDR 40–50 d.c. current supply is used to impose the cell current (constant current operations). The anolyte flow velocity $\bar{v}_a$ is always equal to $\bar{v}_c$, except when $\bar{v}_c = 5$ cm s^{-1}, case for which $\bar{v}_a = 3$ cm s^{-1}.

3. Experimental results

3.1. *Visual observations*

As the wall is transparent, visual observations of the gas evolving cathodes are possible when expanded metal is used for these electrodes. These may be summarized as follows:

(a) when the small diagonal CD is parallel to the electrolyte flow direction (cases b-1 and b-2), there is coalescence of bubbles and trapping of large bubbles which escape upwards from time to time (see Fig. 3a).

(b) for any orientation of the mesh, an almost homogeneous curtain of bubbles exists along the cathode (see Fig. 3b) when small currents are imposed. At currents higher than 3 A, there is a dense section of the bubble curtain, the lower position and the height, Y_R, of which depend on $\bar{v}_c$ and on I. When $\bar{v}_c$ is increased, the lower limit of the dense curtain moves towards the top of the electrode; the height Y_R increases with the intensity I of the current.

3.2. *Cell voltage*

Fig. 4 gives three representations of experimental results obtained with material M2 (Figs. 4a and c) and with the micromesh (Fig. 4b). The cell voltage U_c is approximately proportional to the current I whatever the velocity $\bar{v}_c$, and a planar electrode always produces a higher increase of U_c with I (Fig. 4a). When large bubbles are formed and temporarily immobilized within the structure of the electrode just in front of the separator (Fig. 2c, i.e. orientation b-1), U_c is higher than when the diverting effect is acting away from the separator (orientation b-2) or when the orientation of Fig. 2a is used. For the micromesh (Fig. 4b) there is no measurable effect of the orientation of the mesh with respect to $\bar{v}_c$, probably because the mesh is relatively small and also the evolved bubbles escape with difficulty owing to the small thickness of the cathodic compartment.
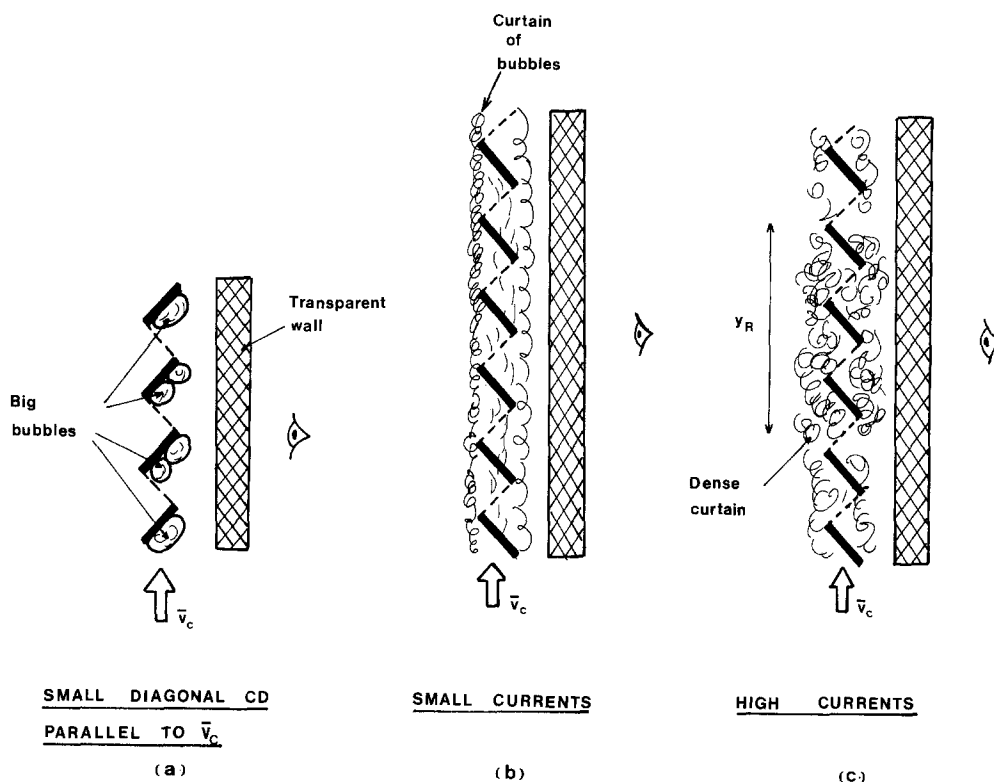
Fig. 3. Typical results of the observations through the wall.

For a given material, there is no evident effect of the electrolyte velocity $\bar{v}_c$ on U_c, at least within the range of variation of $\bar{v}_c$; only for orientation b-1 is there a small effect at small values of $\bar{v}_c$. The work of Hine [1], which concerns an expanded metal electrode 100 cm high, showed that there is a small decrease of U_c when $\bar{v}_c$ is increased, as for the case of a planar electrode, but the values given to $\bar{v}_c$ in that work are nearly 400 times higher than in the present study. Hine also comments that there is no significant difference between the behaviour of a planar electrode and an expanded metal electrode because the electrolyte velocity is very high.

In the present study stainless steel and nickel planar electrodes behave differently (U_c is higher for the stainless steel electrode), probably because the bubbles evolved on both materials have different characteristics and in particular different diameters.

3.3. Potential distribution along the electrode

The probes indicated in Fig. 1b have been used to measure the local solution potential in the median plane of the expanded metal or in the plane of the planar cathodes. It is important to mention that when gas is evolving, there is no sensible effect of the lateral position of the extremity of the capillary on the solution potential measured, but the reproducibility of the results is bad owing to the variations of the state of the electrode surface with time. The solution potential measured with probes nos. 2 to 4 is referred to the solution potential given by probe no. 1 which is near the cell entrance; the difference, $\Delta\phi_s$, obtained is represented as a function of the distance y along the electrode height. The metal potential is constant, as shown in separate experiments on the electronic conduction of the electrode material [7].
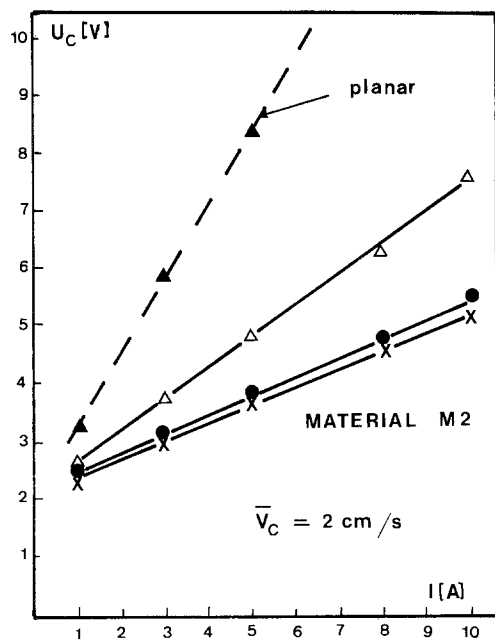
(a)
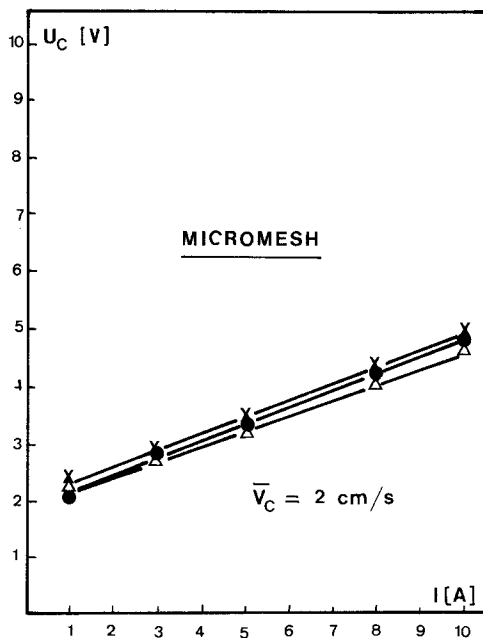
(b)
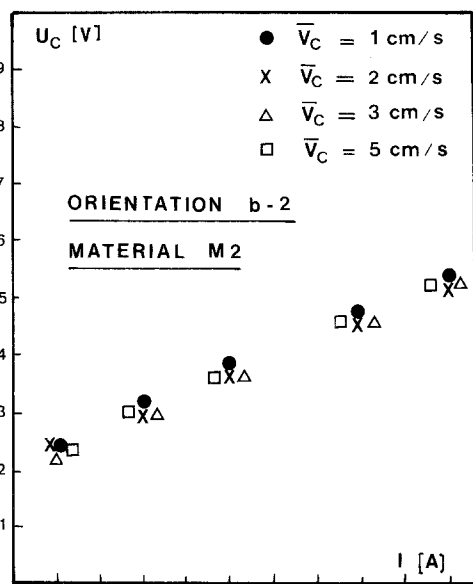
(c)

Fig. 4. Variations of the cell voltage with I and $\bar{v}_c$ for various materals and orientations. For (a) and (b), — — — planar (stainless steel). Expanded metal; △ orientation b-1, × orientation b-2, ● orientation a.

3.3.1. Planar electrodes. Depending on the material (nickel or stainless steel) the solution potential distribution is very different [7]; it also depends on the catholyte velocity and on the current intensity. However, the reproducibility is so poor, particularly for stainless steel, that the pre-

sent presentation is restricted to results obtained with a nickel electrode at a given value of $\bar{v}_c$ (Fig. 5). As y increases from zero, the solution potential difference $\Delta\phi_s$ first increases and then decreases and there is a marked influence of current intensity, particularly near the top of the cell.
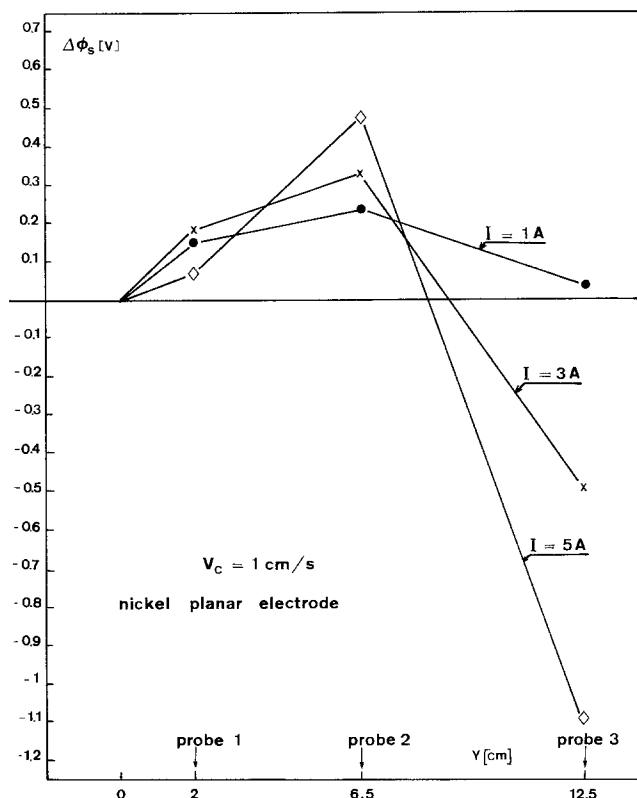
Fig. 5. Variation of the solution potential along the planar electrode.

Results such as those of Fig. 5 may indicate the form of the local current density distribution along the electrode and may be related to a change in the structure of the gas liquid mixture along the sheet. Due to the very bad reproducibility, quantitative conclusions cannot be drawn. Let us recall that it is well known that the superficial state of the electrode varies as the activation of the electrode changes during the experiment, particularly with nickel; the distribution of the nucleation centres and the growth of the bubble both depend directly on the superficial state.

3.3.2. Expanded metal electrodes. Potential distributions have been measured for the three materials and for various flow rates and current intensities [7]. Again owing to the low reproducibility, only qualitative conclusions may be drawn, because the potential distribution changes with time though the form of the distribution is maintained. Figs. 6
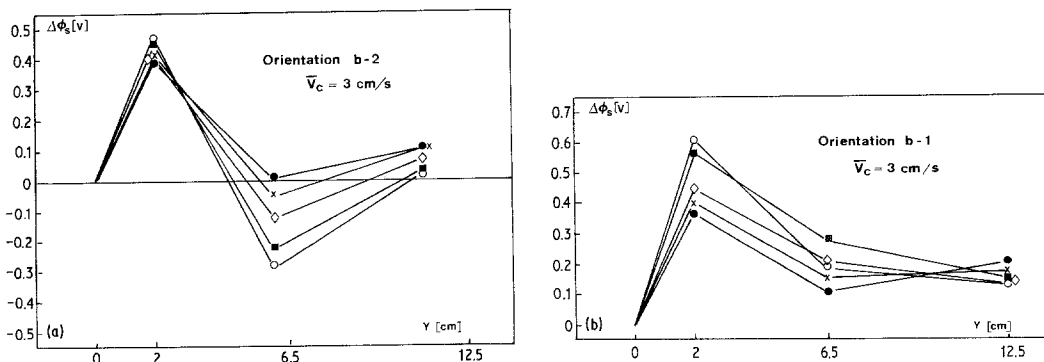

Fig. 6. Variation of the solution potential with I along expanded metal electrodes: (a) orientation b-2, (b) orientation b-1. Material M_2; $\bullet I = 1A$, $\times I = 3A$, $\Diamond I = 5A$, $\blacksquare I = 8A$, $\circ I = 10A$.
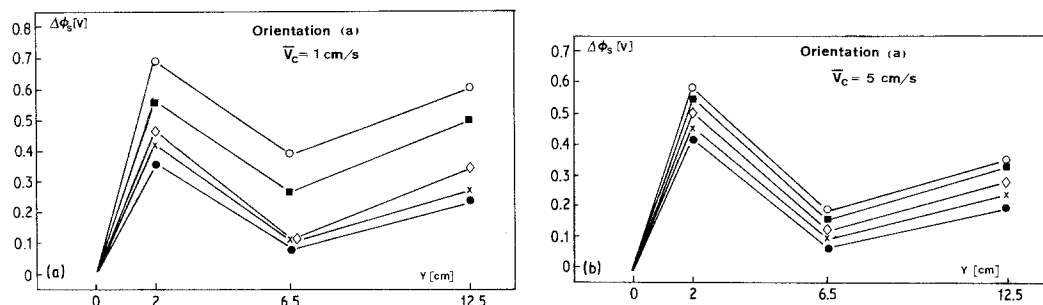
Fig. 7. Variation of the solution potential with I along expanded metal electrodes orientation (a). Material M_2; $\bullet I = 1A$, $\times I = 3A$, $\Diamond I = 5A$, $\blacksquare I = 8A$, $\circ I = 10A$.

and 7 are given as examples for material M2.

When the mesh of the expanded metal is positioned according to orientation (a), the solution potential changes considerably along the electrode; also, at a given position, the increase of $\bar{v}_c$ reduces the extent of the variation of $\Delta\phi_s$ with I (Figs. 6a and b). The changes of gradient of the plots may reflect variations in the structure of the two-phase system. As I is increased the potential difference is also increased.

The form of the distributions changes with a change of the orientation of the same material, as shown by Figs. 6a and b. When the immobilization of large bubbles within the structure may affect the primary current distribution (Fig. 6b), the form of the potential distribution is different from that when the bubbles are immobilized in the back side of the electrode (Fig. 6a). The interpretation of such distributions is complex because they are possibly related to the existance of a dense curtain of bubbles at high values of I and with the geometrical variation of this curtain when the parameters are changed. A lot of results have been obtained for material M_1 and also for micromesh, with distributions similar to those of Figs. 5 and 6: these are also difficult to interpret.

4. Discussion

As can be observed in the literature, the few studies on vertical gas evolving electrodes of expanded metal do not take into account the orientation of the mesh relative to the general electrolyte flow direction. However, it has been seen that this orientation may influence the overall cell voltage and the potential distribution (and hence

the current density distribution) owing to the fact that the deflecting effect of the gas–liquid mixture depends on that orientation. Configuration (a) (LD parallel to $\bar{v}_c$) does not favour the coalescence of bubbles, contrary to the two other orientations, and can be recommended.

The visual observations emphasize the existence of a dense curtain of bubbles around the expanded metal electrode. The advantage of the expanded metal compared to a planar electrode, is its ability to deflect the gas towards the rear side of the electrode.

With expanded metal, it is difficult to imagine sectioned electrodes or micro-electrodes for the experimental determination of the local current density distribution. Thus, the study of the potential distribution with probes is a possible means of obtaining an indication of the c.d. distribution.

The electrodes used in the present work are very short (14 cm) compared to gas evolving electrodes (100 cm) encountered in vertical industrial cells. But the aim here was to call attention to the effectiveness of the expanded metal and to the importance of the orientation of the mesh with respect to the gas–liquid flow.

5. Conclusion

Besides visual observations which show different aspects of the gas–liquid mixture, the experiments show that the cell voltage depends on the orientation of the mesh of the expanded metal. Given orientations make possible the deflecting effect of the gas–liquid mixture but at the same time they facilitate the coalescence of bubbles and the immobilization of big bubbles. The solution potential distributions along different electrodes present

variations which are probably due to the structure of the two-phase system.

Acknowledgement

References

[1]   F. Hine, M. Yasuda, Y. Ogata and K. Hara, *J. Electrochem. Soc.* **131** (1984) 83.

[2]   J. Jorne and J. F. Louvar, *ibid.* **127** (1980) 298.
[3]   L. J. Janssen, J. J. M. Geraets, E. Barendrecht and D. S. J. van Stralen, *Electrochim. Acta* **27** (1982) 1207.
[4]   F. Hine and K. Murakami, *J. Electrochem. Soc.* **128** (1981) 64.
[5]   *Idem, ibid.* **127** (1980) 292.
[6]   F. Hine, M. Yasuda, R. Nakamura and T. Noda, *ibid.* **122** (1975) 1185.
[7]   C. Elsner, Thesis, University of Rennes, (1984).